PCCP

The Fundamental Vibrational Frequencies and Spectroscopic Constants of the $C_2O_2H_2$ Isomers: Molecules Known in Simulated Interstellar Ice Analogues

Journal:	*Physical Chemistry Chemical Physics*
Manuscript ID	CP-ART-05-2024-002201.R2
Article Type:	Paper
Date Submitted by the Author:	20-Jul-2024
Complete List of Authors:	Watrous, Alexandria; University of Mississippi, Chemistry & Biochemistry Fortenberry, Ryan; University of Mississippi, Department of Chemistry & Biochemistry

PCCP

ARTICLE TYPE

Cite this: DOI: 00.0000/xxxxxxxxxx

The Fundamental Vibrational Frequencies and Spectroscopic Constants of the $C_2O_2H_2$ Isomers: Molecules Known in Simulated Interstellar Ice Analogues†

Alexandria G. Watrous[a] and Ryan C. Fortenberry*[a]

Received Date
Accepted Date

DOI: 00.0000/xxxxxxxxxx

While *trans*-glyoxal may not be easily observable in astronomical sources through either IR or radioastronomy due to its C_{2h} symmetry, its *cis* conformer along with the *cyc*-H_2COCO epoxide isomer should be ready targets for astrochemical detection. The present quantum chemical study shows that not only are both molecular isomers strongly polar, they also have notable IR features and low isomerisation energies of 4.1 kcal mol^{-1} and 10.7 kcal mol^{-1}, respectively. These three isomers along with two other $C_2O_2H_2$ isomers have had their full set of fundamental vibrational frequencies and spectroscopic constants characterised herein. These isomers have previously been shown to occur in simulated astrophysical ices making them worthy targets of astronomical search. Furthermore, the hybrid quartic force field (QFF) approach utilized herein to produce the needed spectral data has a mean absolute percent error compared to the experimentally-available, gas phase fundamental vibrational frequencies of 0.6% and rotational constants to better than 0.1%. The hybrid QFF is defined from explicitly correlated coupled cluster theory at the singles, doubles, and perturbative triples level [CCSD(T)-F12b] including core electron correlation and a canonical CCSD(T) relativity correction for the harmonic (quadratic) terms in the QFF and simple CCSD(T)-F12b/cc-pVDZ energies for the cubic and quartic terms, the so-called "F12-TcCR+DZ QFF," and is producing spectroscopically-accurate predictions for both fundamental vibrational frequencies and principal spectroscopic constants. Hence, the values computed in this work should be notably accurate and, hence, exceptionally useful to the spectroscopy and astrochemistry communities.

1 Introduction

Ices are likely reservoirs for all sorts of interstellar complex organic molecules (iCOMs).[1–6] They form slowly over time, are hit on occasion by high-energy photons as well as relativistic particles, but are otherwise largely isolated from other bodies. Hence, these materials are veritable playgrounds for novel and "otherworldly" chemistry. Most of the upper layers of these ices are composed of volatiles typically including condensed and amorphous water, carbon mono-/dioxide, methanol, and some sprinkling of other molecules like ammonia, formaldehyde, and such related materials.[7–9] The interactions of these particles over the eons can then lead to novel molecules which can, in turn, desorb off the surface of the icy grains. These desorbed molecular species are then astronomically detectable and can add to the current census of known interstellar molecules.[10,11]

This hypothesis of ice phase chemistry followed by gas phase desorption as one of many routes for the production of observed molecules in various astronomical environments holds through a combination of molecular modeling[12–15] and simulated laboratory experiments[6,16,17] combined with how these two items help to explain observed astrochemical phenomena.[7,18] The resulting interconnected triangle of astrochemistry is the foundation for how the chemical cosmos can be interpreted. Many of the experiments undertaken to define one end of this astrochemical triangle are constructed with layers of organic material set down on a cold finger in near-vacuum. The organic residue is, then, hit with some form of energy either through an electric arc, high-energy photons, or some type of molecular beam. The materials that are desorbed can be detected through mass spectrometery and/or infrared spectroscopy. Within such experiments, organic molecules that are common on Earth have also been detected including those that add flavor to chocolate or buttered popcorn[19,20] as fun examples, but many are much more exotic. However, recent work has shown that ice comprised of carbon monoxide and water irradiated with 5 keV electrons has produced glyoxal (*trans*-OCHHCO),[21] the simplest dialdehyde and a common industrial chemical for paper coatings and clothing starches. While glyoxal

[a] University of Mississippi, University, MS, US; E-mail: r410@olmiess.edu

† Electronic Supplementary Information (ESI) available: [details of any supplementary information available should be included here]. See DOI: 10.1039/cXCP00000x/

is a well-known industrial molecule, this interstellar ice simulation also produces what appears to be all of its $C_2O_2H_2$ structural and conformational isomers, as well. From a structural perspective, one of the most interesting is acetylenediol (HOCCOH) due to its alcohol-terminated ends of acetylene, as one example. These experiments follow recent work where similar experiments produce the related ethnyol (HCCOH) molecule, a higher-energy isomer of ketene (H_2CCO).[22]

The presence of these $C_2O_2H_2$ molecular isomers in simulated interstellar ices combined with the possibility that they may desorb into the gas phase clearly shows that spectral reference data need to be available for their possible detection, especially in the age of the *James Webb Space Telescope* (JWST) and the Atacama Large Millimeter Array (ALMA) observing in the IR and radio, respectively. The gas phase fundamental vibrational frequencies producing the IR spectrum for the *trans* form of glyoxal have been known for the better part of over 50 years,[23–26] but the other isomers only have a few fundamentals previously reported. Many of these are from Ar-matrix experiments or relatively low-level quantum chemical computations. The rotational spectroscopic constants for *cis*-glyoxal are also available in the literature,[27] but spectral data for the other $C_2O_2H_2$ isomers are largely unknown.

As such, the present work will fill in the knowledge gap for these molecules and will provide accurate spectroscopic classification for the five lowest-energy, $C_2O_2H_2$ isomers in a manner similar to that for ethynol,[22,28] methanediol,[16,29,30] and diaminomethane.[31,32] The existence of the *trans*-glyoxal gas phase, experimental fundamental vibrational frequencies will allow for benchmarking of the employed quantum chemical methods, and such findings will give clear error expectations for the fundamental frequencies and spectroscopic constants for the other computed isomers. The present approach in this work will employ the venerable quartic force field (QFF) for approximating the anharmonic potential about the minimum and will be conjoined to second-order rotational and vibrational perturbation theory (VPT2).[33–36] Such approaches are notable for their applicability to providing reference data from *ab initio* quantum chemical computations[37–41] and have aided in the recent detection of several novel molecules in the laboratory as well as in astronomical environments.[42–50] As such, the data provided in this work should be able to guide future gas phase experimental searches for these molecules and could possibly also help to inform astronomical searches, if the computational results are accurate enough.

2 Computational Details

QFFs are fourth-order Taylor series expansions. In this case, they are expanding the potential portion of the internuclear Watson Hamiltonian. QFFs are specific types of potential energy surfaces and are defined for the present work based on the level of electronic structure theory utilized to compute the corresponding energy points for the level of theory employed. For the present work, the geometries of the five isomers of $C_2O_2H_2$ are, first, optimized using coupled cluster theory at the singles and doubles level with the addition of perturbative triples [CCSD(T)],[51–53] the "gold-standard" of quantum chemistry,[54] within the explicitly correlated (F12b) formalism[55,56] as available within the MOLPRO quantum chemistry program.[57,58] CCSD(T)-F12b is paired with the core-correlating, correlation consistent triple-ζ basis set (cc-pCVTZ).[59]

From this reference geometry, the PBQFF program[60] is employed to define normal coordinates for each isomer and computes the QFF using the CCSD(T)-F12b/cc-pCVTZ-F12 level of theory with a composite correction included for scalar relativity via the Douglas-Kroll Hamiltonian[61] with canonical CCSD(T)/cc-pVTZ-DK computations for the relativity turned on and turned off. The use of these terms produces the so called "F12-TcCR" QFF[62] for inclusion of triple-ζ (T), core electron correlation (cC) as well as relativity (R) in the composite energy. The PBQFF program, then, further employs VPT2 in an updated, Rust-written version of the SPECTRO program[63] where Fermi-resonance polyads are included within the computation and affect the reported frequencies; these are listed in the electronic supplementary information (ESI). Additionally, a hybrid QFF is also examined in this work where the harmonic terms are computed with F12-TcCR, and the anharmonic terms are computed simply with CCSD(T)-F12b/cc-pVDZ-F12 giving the "F12-TcCR+DZ" QFF. The latter has been shown to produce similar accuracy to F12-TcCR but for 25% of the computational cost.[64] In turn, F12-TcCR is known to be just as accurate as the previous generation of composite QFFs computed in a similar manner[65–68] but for only 4% of the computational cost.

The dipole moments are computed via CCSD(T)-F12b/cc-pVTZ-F12, called "F12-TZ" herein, and the Cartesian vectors for the dipole moments are given in the ESI. The vibrational intensities are computed with B3LYP/aug-cc-pVTZ as available within the Gaussian16 program[69–73] and are known to be comparable with those derived from larger, semi-global dipole moment surfaces.[74,75] Anharmonic intensities are also reported for the two-quanta overtones and combination bands where the intensities are on the order of 10 km mol^{-1} or larger. The term "out-of-plane bend" is replaced herein with "OPB" and "in-plane bend" with "IPB." All of the rotational constants are computed in the Watson A-Reduced Hamiltonian unless otherwise noted.

3 Results & Discussion

The structures and relative energies for the five isomers are given in Fig. 1. The relative energies are from F12-TcCR minima with anharmonic zero-point vibrational energies included. The relative energies are similar to those computed previously,[21,76] but these include further corrections for core electron corrlation, relativity, and anharmonic zero-points making them the most accurate relative energies computed to date for the $C_2O_2H_2$ isomers. The peroxide isomer is not included in this study as it lies significantly higher in energy ($>\sim$ 100 kcal mol^{-1}) than the other five, and O−O bonds are typically weak. In any case, clearly the glyoxal, dialdehyde isomers are the lowest in energy with the rotationally-active, C_{2v}, *cis* isomer being 4.1 kcal mol^{-1} higher in energy than the *trans* global minimum. The cyclic isomer and ketone step up in energy compared to the dialdehydes, but they are within 20 kcal mol^{-1} of *trans*-glyoxal. The diol is notably higher and exihibits C_2 symmetry with O−C−C bond angles of nearly but not quite 180°. Such a structure is exceptionally difficult to optimize

Table 1 Vibrational frequencies (in cm^{-1}) of *trans*-glyoxal with B3LYP/aug-cc-pVTZ intensities (f in km mol^{-1})

Mode	Description	F12-TcCR	F12-TcCR+DZ	F12-CTZ	f	Expt.
ω_1 (a_g)	Sym C−H Stretch	2994.7	2994.7	2995.4	–	
ω_2 (b_u)	Anti-Sym C−H Stretch	2991.2	2991.2	2992.0	94	
ω_3 (a_g)	Sym C−O Stretch	1783.6	1783.6	1785.7	–	
ω_4 (b_u)	Anti-Sym C−O Stretch	1765.9	1765.9	1767.9	127	
ω_5 (a_g)	Sym C−H Rock	1383.7	1383.7	1384.6	–	
ω_6 (b_u)	Anti-Sym C−H Rock	1343.0	1343.0	1344.2	6	
ω_7 (a_g)	C−C Stretch	1099.4	1099.4	1099.9	–	
ω_8 (b_g)	Anti-SymC−H Wag	1067.6	1067.6	1069.2	–	
ω_9 (a_u)	Sym C−H Wag	814.9	814.9	816.1	3	
ω_{10} (a_g)	Sym C−C−O Bend	562.0	562.0	562.4	–	
ω_{11} (b_u)	Anti-Sym C−C−O Bend	335.7	335.7	336.0	50	
ω_{12} (a_u)	Torsion	129.5	129.5	130.1	34	
ν_1 (a_g)	Sym C−H Stretch	2838.8	2835.3	2845.0	–	2843[a]
ν_2 (b_u)	Anti-Sym C−H Stretch	2842.5	2830.0	2840.0	100	2835.07[b]
ν_3 (a_g)	Sym C−O Stretch	1751.8	1749.8	1757.4	–	1745[a]
ν_4 (b_u)	Anti-Sym C−O Stretch	1714.2	1744.0	1711.0	114	1732[b]
ν_5 (a_g)	Sym C−H Rock	1352.8	1351.4	1362.0	–	1338[c]
ν_6 (b_u)	Anti Sym C−H Rock	1321.1	1315.6	1318.4	6	1312.4[b]
ν_7 (a_g)	C−C Stretch	1078.2	1061.8	1081.8	–	1065[a]
ν_8 (b_g)	Anti-Sym C−H Wag	974.1	1058.7	997.3	–	1047.91[a]
ν_9 (a_u)	Sym C-H Wag	773.9	806.3	803.9	2	801.4[b]
ν_{10} (a_g)	Sym C−C−O Bend	532.2	544.0	566.8	–	550.53[d]
ν_{11} (b_u)	Anti-Sym C−C−O Bend	351.2	338.1	419.6	49	338.6[b]
ν_{12} (a_u)	Torsion	129.5[e]	125.3	151.6	32	126.6[b]
$\nu_3+\nu_4$			3468.7		10	
$\nu_6+\nu_{11}$			1653.6		9	

[a]Experimental data from Ref. 24
[b]Experimental gas phase data from Ref. 23
[c]Experimental Raman data from Ref. 25
[d]Experimental data from Ref. 26
[e]Harmonic value used due to problems with this mode.

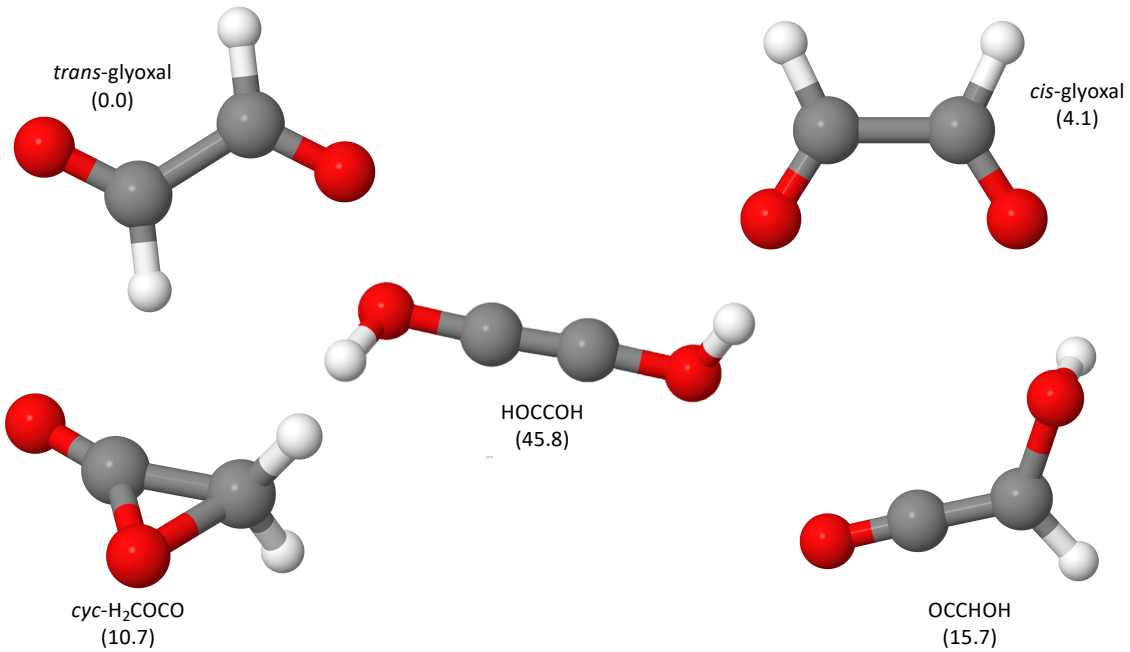

Fig. 1 Optimized geometries and relative energies (in parentheses in kcal mol^{-1}) for the $C_2O_2H_2$ isomers with names of the molecules given. O (red), C (gray), and H (white).

Table 2 Rotational Constants of *trans*-glyoxal

Const.	Units	F12-TcCR	F12-TcCR+DZ
A_e	MHz	56028.7	56028.7
B_e	MHz	4819.8	4819.8
C_e	MHz	4438.0	4438.0
A_0	MHz	55321.9	55311.3
B_0	MHz	4798.2	4797.8
C_0	MHz	4416.7	4416.3
Δ_J	kHz	1.188	1.188
Δ_K	kHz	511.950	511.950
Δ_{JK}	kHz	−7.583	−7.583
δ_J	Hz	118.287	118.287
δ_K	kHz	6.178	6.178[a]
Φ_J	μHz	169.256	160.173
Φ_K	Hz	13.064	13.073
Φ_{JK}	mHz	−6.109	−6.363
Φ_{KJ}	mHz	−734.361	−735.701
ϕ_j	μHz	82.721	81.823
ϕ_{jk}	mHz	2.302	2.185
ϕ_k	Hz	1.016	1.015[b]
κ		−0.985	

[a]Within the S-reduced Hamiltonian, $d_2 = -5.726$ Hz.
[a]Within the S-reduced Hamiltonian, $h_3 < 1$ mHz.

due to the near linearity of the four heavy atoms and the problems this causes with the subsequent dihedral angle definitions. Even so, the present computations put the O−C−C bond angles at 176.743°. Again, these molecules, regardless of their relative energies, have been generated in laboratory simulations of astrochemical ices,[21] and their spectral data may help to explain spectral features of regions where ices are known to form.

As shown in Table 1, most of the presently computed, quantum chemical, F12-TcCR QFF VPT2 anharmonic frequencies are in good agreement with experiment. The mean absolute percent error (MA%E) is 2.1% compared to experiment. For example, the frequency for ν_1 is computed to be 2838.8 cm^{-1} with experiment at 2843 cm^{-1},[24] a percent error of just 0.4%. The main outlier for the F12-TcCR anharmonic fundamental frequencies is ν_8 which is computationally predicted to be nearly 74 cm^{-1} less than the experimental value of 1047.91 cm^{-1}.[24] The rest are within 19 cm^{-1} of expeirment. Furthermore, the ν_{12} frequency is computed to produce a non-physical negative frequency. Hence, the harmonic value is retained in Table 1 as it is already within 3.0 cm^{-1} of experiment. Such erroneous behavior is emerging in computations of this type where some lower frequency fundamentals experience numerical instability in the cubic and quartic terms.

The best solution appears to be imposing a hybrid QFF, F12-TcCR+DZ in this case. F12-TcCR+DZ maintains the accuracy in the dominant harmonic terms but utilizes the numerical stability of the non-composite F12-DZ single-point energies for the cubic and quartic terms. Additionally, F12-DZ is effectively canonical CCSD(T)/aug-cc-pVQZ,[77] and surprisingly effective treatment of vibrational and rotational constants with F12-DZ has been benchmarked previously.[62] Additionally, numerical instability in the anharmonic terms has also been reported of late,[78] with such hybrid methods discussed as potential means to alleviate such issues.[79] The MA%E of the F12-TcCR+DZ QFF is lower at a nearly trivial 0.6% for the entire set with ν_8 computed to be much closer to experiment at 1058.7 cm^{-1}, an error of 1.0%, the largest of the *trans*-glyoxal fundamental frequencies. All F12-TcCR+DZ QFF frequencies are within 11.0 cm^{-1} of experiment, half of them within 5.0 cm^{-1} or better. The ν_{11} fundamental (338.6 cm^{-1}) is even within 0.5 cm^{-1} of experiment.[23] Hence, the VPT2 fundamental frequencies predicted for the other isomers with the F12-TcCR QFF should be good, but the F12-TcCR+DZ QFF should be better. Additionally, the computed numerical intensities computed herein match the qualitative descriptions (i.e. a "strong" band at 1732 cm^{-1} computed here to be 114 km mol^{-1}) from experiment, as well.

Another alternative is to throw out the relativistic corrections altogether from the QFF and rely solely upon the CCSD(T)-F12b/cc-pCVTZ (F12-CTZ) portion of the energy term as the QFF. The frequencies for this approach are also shown in Table 1. The harmonic frequencies never vary by more than 3.0 cm^{-1} compared to either F12-TcCR or the hybrid QFF, typically by less than 2.0 cm^{-1}. However, the anharmonic terms begin to show larger deviations. The F12-TcCR+DZ QFF fundamentals, for the most part, are closer to experiment than those from the F12-CTZ QFF making them more desirable on-the-whole. Additionally, the added computational cost, roughly an order of magnitude,[62,64,80] gives further support to choosing the hybrid QFF over one computed from F12-CTZ.

The rotational constants for *trans*-glyoxal are given in Table 2. The F12-TcCR and F12-TcCR+DZ spectroscopic constants are effectively identical. They should be for the I^r representation quartic and sextic distortion constants as these are computed at the harmonic level. The anharmonic terms do not greatly influence the zero-point corrected princpal A_0, B_0, and C_0 rotational constants; the large A_0 only shifts by 10.6 MHz for instance. Hence, the rotational constants for either QFF should be equally useful. While this molecule is rotationally inactive due to its C_{2h} symmetry, these rotational constants may aid in constructing a complete partition function for this molecule or provide insights in Raman or rovibrational spectroscopy. They also show that *trans*-glyoxal is near-prolate with $\kappa = -0.985$. B_0 and C_0 differ by 381.5 MHz. The full set of vibrationally-excited rotational constants are given in the (ESI).

The other, C_{2v} dialdehyde isomer, *cis*-glyoxal lying 4.1 kcal mol^{-1} above the *trans* minimum, is rotationally active and much more vibrationally active due to a lack of an inversion center as one of the symmetry operators in its point group. For instance, the ν_1 symmetric C-H stretch and the ν_4 symmetric C-O stretch both have notable intensities in the range of 130 km mol^{-1} as shown in Table 3, nearly double the intensity of the antisymmetric stretch of water. The F12-TcCR+DZ QFF ν_1 is computed herein to be 2831.4 cm^{-1} or right above 3.5 μm nearly adjoining the C-H stretching frequencies in polycyclic aromatic hydrocarbons (PAHs).[81] The ν_1 frequency is also close to the ν_2 anti-symmetric C-H stretch in *cis*-glyoxal of 2812.3 cm^{-1}. Hence, any interstellar glyoxal of either form will likely not be observed in this wavelength region of the IR via JWST, as they will be covered up by PAH features. The ν_4 fundamental is computed to be 1752.9 cm^{-1} for the *cis*, and the same motion for the *trans* (1732 cm−1

Table 3 Vibrational Frequencies (in cm^{-1}) of *cis*-glyoxal with B3LYP/aug-cc-pVTZ intensities (in km mol^{-1})

Mode	Description	F12-TcCR	F12-TcCR+DZ	f
ω_1 (a_1)	Sym C−H Stretch	2961.0	2961.0	175
ω_2 (b_2)	Anti-Sym C−H Stretch	2933.8	2933.8	45
ω_3 (b_2)	Anti-Sym C−O Stretch	1803.9	1803.9	52
ω_4 (a_1)	Sym C−O Stretch	1772.9	1772.9	130
ω_5 (a_1)	Sym O−C−H Bend	1403.0	1403.0	1
ω_6 (b_2)	Anti-Sym O−C−H Bend	1396.5	1396.5	1
ω_7 (a_2)	Anti-Sym C−C OPB	1068.1	1068.1	-
ω_8 (a_1)	C−C Stretch	852.3	852.3	14
ω_9 (b_2)	Anti-Sym C−C IPB	826.3	826.3	74
ω_{10} (b_1)	Sym C−C OPB	741.7	741.7	1
ω_{11} (a_1)	Sym O−C Rocking	282.6	282.6	6
ω_{12} (a_2)	Torsion	86.7	86.6	-
ν_1 (a_1)	Sym C−H Stretch	2813.5	2831.4	130
ν_2 (b_2)	Anti-Sym C−H Stretch	2756.0	2812.3	27
ν_3 (b_2)	Anti-Sym C−O Stretch	1765.2	1777.1	57
ν_4 (a_1)	Sym C−O Stretch	1740.7	1752.9	130
ν_5 (a_1)	Sym O−C−H Bend	1373.5	1366.0	1
ν_6 (b_2)	Anti-Sym O−C−H Bend	1285.8	1370.0	1
ν_7 (a_2)	Anti-Sym C−C OPB	1020.4	1053.8	-
ν_8 (a_1)	C−C Stretch	806.6	824.7	13
ν_9 (b_2)	Anti-Sym C−C IPB	640.2	802.9	52
ν_{10} (b_1)	Sym C−C OPB	656.9	749.5	1
ν_{11} (a_1)	Sym O−C Rocking	247.8	266.8	6
ν_{12} (a_2)	Torsion	−348.8	348.0	-
$2\nu_2$			2710.3	47
$\nu_5+\nu_6$			2680.8	22
$\nu_{10}+\nu_{12}$			1169.5	19

Table 4 Rotational Constants and Dipole Moment (F12-TZ) for *cis*-glyoxal

Const.	Units	F12-TcCR	F12-TcCR+DZ	Exp.[a]
A_e	MHz	26672.0	26672.0	
B_e	MHz	6265.4	6265.4	
C_e	MHz	5073.6	5073.6	
A_0	MHz	26757.9	26737.3	26713.366(3)
B_0	MHz	6183.1	6188.7	6190.8042(6)
C_0	MHz	5030.0	5033.0	5032.4513(5)
Δ_J	kHz	6.192	6.192	6.368(1)
Δ_K	kHz	169.836	169.832	192.41(2)
Δ_{JK}	kHz	−44.785	−44.781	−48.07(1)
δ_J	kHz	1.623	1.623	1.7006(2)
δ_K	kHz	12.962	12.960	16.39(2)
Φ_J	mHz	8.327	8.670	6.0(9)
Φ_K	Hz	6.223	6.178	9.2(2)
Φ_{JK}	mHz	140.848	135.302	125.(13)
Φ_{KJ}	Hz	−2.075	−2.045	−2.52(50
ϕ_j	mHz	3.953	4.069	1.98(9)
ϕ_{jk}	mHz	18.437	19.489	−73.(16)
ϕ_k	Hz	1.633	1.635	
μ	D	3.55		
κ		−0.894		

[a] Gas phase experimental data from Ref. 27

Table 5 Vibrational frequencies (in cm^{-1}) of *cyc*-H_2COCO with B3LYP/aug-cc-pVTZ intensities (in km mol^{-1})

Mode	Description	F12-TcCR	F12-TcCR+DZ	f	Expt.
ω_1 (a'')	Anti-Sym C−H Stretch	3251.6	3251.6	1	
ω_2 (a')	Sym C−H Stretch	3144.4	3144.4	3	
ω_3 (a')	C−O Stretch	2003.6	2003.6	454	
ω_4 (a')	C−H−H Bend	1490.4	1490.4	1	
ω_5 (a')	C−H−H Bend	1206.1	1206.1	9	
ω_6 (a')	C−O Stretch	1115.3	1115.3	70	
ω_7 (a'')	C−H−H Wag	1064.7	1064.7	1	
ω_8 (a'')	Anti-Sym C−H−H Rock	1009.1	1009.1	2	
ω_9 (a')	Sym C−H−H Rock	963.8	963.8	75	
ω_{10} (a')	C−C−O IPB	717.1	717.1	41	
ω_{11} (a')	C−C−O IPB	535.6	535.6	7	
ω_{12} (a'')	O−C−O OPB	489.3	489.3	5	
ν_1 (a'')	Anti-Sym C−H Stretch	3102.4	3099.5	1	
ν_2 (a')	Sym C−H Stretch	3020.6	3019.4	3	
ν_3 (a')	C−O Stretch	1966.4	1963.0	290	1960 ± 2[a] 1967[b]
ν_4 (a')	C−H−H Bend	1440.7	1441.4	1	
ν_5 (a')	C−H−H Bend	1168.5	1172.0	6	
ν_6 (a')	C−O Stretch	1088.8	1085.6	63	
ν_7 (a'')	C−H−H Wag	1039.0	1044.3	1	
ν_8 (a'')	Anti-Sym C−H−H Rock	983.7	988.6	2	
ν_9 (a')	Sym C−H−H Rock	934.8	936.0	58	
ν_{10} (a')	C−C−O IPB	691.1	689.4	42	
ν_{11} (a')	C−C−O IPB	526.3	526.1	6	
ν_{12} (a'')	O−C−O OPB	480.4	492.9	4	
$\nu_6+\nu_8$			2214.2	29	
$\nu_5+\nu_8$			2155.8	44	
$\nu_5+\nu_9$			2111.6	11	
$2\nu_8$			1979.0	166	
$2\nu_9$			1854.5	45	
$2\nu_{12}$			995.3	11	

[a] Experimental gas phase data from Ref. 84
[b] Experimental CO_2 matrix data from Ref. 85

from experiment; 1744.0 cm^{-1} from the F12-TcCR+DZ QFF) also falls in a PAH band at 5.7 μm. Again, this PAH region is dominated by combination bands implying that strong fundamentals of an abundant molecule may yet be discernible at such wavelengths. Once more, the F12-TcCR+DZ QFF produces less anharmonic fundamental vibrational frequencies below 1500 cm^{-1} as shown in Table 3 implying from the *cis* benchmark that they should be more reliable. However, only the ν_8 (824.7 cm^{-1}) and ν_9 (802.9 cm^{-1}) fundamentals exhibit any notable intensity.

Differently, *cis*-glyoxal is strongly dipolar (3.55 D), and its rotational spectroscopic constants are given in Table 4. The rotational constants are showcasing exceptional accuracy compared to previous experiment. The C_0 F12-TcCR+DZ value of 5033.0 MHz is within 1.0 MHz of experiment at 5032.4513 MHz,[27] and B_0 is within 2.1 MHz of experiment. Even the A_0 constant agrees to within 24.0 MHz or less than 0.1%. The quartic and sextic distortion constants are not as accurate, but they are providing semi-quantitative correlation to these values well within their limits.[82,83] Consequently, the F12-TcCR+DZ QFF should be able to predict numerically-accurate, anharmonic fundamental vibrational frequencies and rotational constants for the rest of the isomers of $C_2O_2H_2$ that have yet to be observed spectroscopically in the laboratory and may be present in astronomical environments.[21]

The next, lowest-lying isomer is *cyc*-H_2COCO (α-lactone) which, again, is computed herein to be 10.7 kcal mol^{-1} above

Table 6 Rotational Constants and Dipole Moment (F12-TZ) of *cyc*-H_2COCO

Const.	Units	F12-TcCR	F12-TcCR+DZ
A_e	MHz	25224.8	25224.8
B_e	MHz	8127.9	8127.9
C_e	MHz	6415.5	6415.5
A_0	MHz	24913.3	24910.3
B_0	MHz	8101.9	8102.1
C_0	MHz	6372.8	6372.7
Δ_J	kHz	2.066	2.066
Δ_K	kHz	93.890	93.890
Δ_{JK}	kHz	15.540	15.540
δ_J	Hz	509.335	509.334
δ_K	kHz	12.049	12.049
Φ_J	mHz	1.201	1.208
Φ_K	mHz	−34.889	−47.284
Φ_{JK}	mHz	23.699	23.502
Φ_{KJ}	mHz	156.937	160.112
ϕ_j	μHz	581.845	586.368
ϕ_{jk}	mHz	17.816	17.812
ϕ_k	mHz	782.551	783.981
μ	D	3.31	
κ		−0.813	

Table 7 Vibrational frequencies (in cm^{-1}) of OCCHOH with B3LYP/aug-cc-pVTZ intensities (in km mol^{-1})

Mode	Description	F12-TcCR	F12-TcCR+DZ	f
ω_1 (a)	O−H Stretch	3826.0	3826.0	52
ω_2 (a)	C−H Stretch	3218.6	3218.6	17
ω_3 (a)	C−C Stretch	2187.7	2187.7	506
ω_4 (a)	H−C−O Bend	1434.7	1434.7	18
ω_5 (a)	H−O−C Bend	1280.9	1280.9	38
ω_6 (a)	C−O Stretch	1184.3	1184.3	74
ω_7 (a)	C−C−O Bend	1040.6	1040.6	24
ω_8 (a)	O−C−C IPB	682.1	682.1	6
ω_9 (a)	O−C−H OPB	576.8	576.7	46
ω_{10} (a)	O−C−C OPB	491.9	491.9	26
ω_{11} (a)	H−O−C Bend	277.9	277.9	109
ω_{12} (a)	O−C−O Bend	225.7	225.7	5
ν_1 (a)	O−H Stretch	3635.2	3633.8	35
ν_2 (a)	C−H Stretch	3083.8	3079.4	16
ν_3 (a)	C−C Stretch	2137.8	2137.1	303
ν_4 (a)	H−C−O Bend	1398.8	1391.7	15
ν_5 (a)	H−O−C Bend	1262.0	1247.4	19
ν_6 (a)	C−O Stretch	1180.4	1161.5	40
ν_7 (a)	C−C−O Bend	1010.2	1008.0	15
ν_8 (a)	O−C−C IPB	687.6	673.7	5
ν_9 (a)	O−C−H OPB	535.2	561.0	18
ν_{10} (a)	O−C−C OPB	521.9	482.2	36
ν_{11} (a)	H−O−C Bend	344.4	246.0	54
ν_{12} (a)	O−C−O Bend	374.0	231.9	27
$2\nu_1$			7081.3	11
$\nu_6+\nu_7$			2179.0	180
$\nu_7+\nu_{12}$			1258.8	24
$2\nu_9$			1112.3	16
$2\nu_{10}$			965.9	14
$2\nu_{11}$			462.8	16

the *trans*-glyoxal minimum, very close to the 10.2 kcal mol^{-1} from a CCSD(T)/CBS energy difference from within W2-F12 theory.[76] The *cyc*-H_2COCO structure (as shown in Fig. 1) is an epoxide like the astronomically-observed propylene oxide,[86] but *cyc*-H_2COCO also exhibits a ketone and retains C_s symmetry. This isomer is much closer to the minimum than epoxide is to ketene for the related C_2OH_2 isomers,[22] implying that *cyc*-H_2COCO may likely have much more of a role in the chemistry of related molecules than even the experimentally-known oxirene. Previous unscaled harmonic vibrational frequencies and IR intensities computed at the B3LYP/aug-cc-pVDZ have been reported previously[84] as have scaled harmonic vibrational frequencies from B3LYP/aug-cc-pVTZ.[87] However, the present computations represent a significant improvement in the quantum chemical level of theory employed for computing the vibrational spectral data of this molecule.

Table 5 contains the fundamental vibrational frequencies for *cyc*-H_2COCO. The F12-TcCR and F12-TcCR+DZ QFF anharmonic fundamental frequencies actually are in close alignment for this molecule, agreeing to within 5.0 cm^{-1} in all cases save for ν_{12}. Previous gas phase experimental classification of ν_3 put this frequency at 1960 ± 2 cm^{-1} exceptionally close to the 1963.0 cm^{-1} F12-TcCR+DZ QFF value with the F12-TcCR slightly above this. Hence, these benchmarks are highlighting the accuracy and the reliability for the remaining and previously unattributed fundamental frequencies. The most notable fundamental frequency for *cyc*-H_2COCO is, again, the ν_3 C-O, ketone stretch at 1963.0 cm^{-1}. The reason that this frequency has been observed in both the gas and condensed phases even while originating from such a high energy isomer comes from the notable intensity of this stretch at 290 km mol^{-1}, approaching the level of the antisymmetric stretch in CO_2 in terms of intensity. Additionally, the very close $2\nu_8$ overtone is computed to have an intensity of more than two-thirds as much implying that at low-resolution, there should be a notable combination of intensity here making the combined feature readily observable. The ν_3 fundamental (and possible $2\nu_8$ overtone combination) also is found in a region that is largely bereft of astronomical IR features, especially attributed ones, implying that *cyc*-H_2COCO may be a logical molecular target for future JWST observations. Experimentally, the ν_6 ketone stretch (1085.6 cm^{-1}) and the ν_9 CH_2 rock (936.0 cm^{-1}) will also help to characterize this molecule within the IR.

The rotational constants for *cyc*-H_2COCO are given in Table 6 and show that this isomer is the least prolate of the set. The B and C constants are also the largest of the isomers, but the 3.31 D dipole moment is the second-largest only behind *cis*-glyoxal. As such, the data provided in this work should serve not only as markers for but also motivation for astronomical searches for this molecule.

Little appears to be known about the OCCHOH isomer at 15.7 kcal mol^{-1} above the glyoxal minimum. This C_1 molecule is actually just OH-functionalized ketene, a known interstellar molecule in its own right along with its related radical.[22,88,89] In any case, OCCHOH is also exhibiting a large intensity transition (303 km mol^{-1}) in the range of 4-5 μm for its ν_3 C-C stretch at 2137.1 cm^{-1} for F12-TcCR+DZ; F12-TcCR is within 1.0 cm^{-1} of its counterpart. The $\nu_6+\nu_7$ combination band at 2179.0 cm^{-1} is also exhibiting a notable intensity in this same frequency range as the ν_3 fundamental similar to the close proximity of ν_3 along with $2\nu_8$ for *cyc*-H_2COCO. All other fundamentals are IR active with intensities typically in the 10-40 km mol^{-1}. The F12-TcCR+DZ low frequency values are more anharmonic than the F12-TcCR

Table 8 Rotational Constants and Dipole Moment (F12-TZ) of OCCHOH

Const.	Units	F12-TcCR	F12-TcCR+DZ
A_e	MHz	48596.1	48596.1
B_e	MHz	4709.2	4709.2
C_e	MHz	4347.4	4347.4
A_0	MHz	49079.1	48912.0
B_0	MHz	4680.4	4685.7
C_0	MHz	4318.3	4321.6
Δ_J	kHz	2.510	2.510
Δ_K	MHz	3.670	3.670
Δ_{JK}	kHz	−130.680	−130.689
δ_J	Hz	508.282	508.265
δ_K	kHz	13.886	13.881[a]
Φ_J	mHz	8.784	9.418
Φ_K	Hz	839.650	813.785
Φ_{JK}	mHz	−114.838	−163.068
Φ_{KJ}	Hz	−21.773	−20.041
ϕ_j	mHz	3.061	3.251
ϕ_{jk}	mHz	168.280	178.032
ϕ_k	Hz	29.375	29.651[b]
μ	D	1.98	
κ		−0.984	

[a]Within the S-reduced Hamiltonian, $d_2 = -29.377$ Hz.
[a]Within the S-reduced Hamiltonian, $h_3 < 1$ mHz.

for OCCHOH, but the previous benchmarks imply that the hybrid method should be more representative of physical realty. OCCHOH is also near-prolate ($\kappa = -0.984$; Table 8) and has a dipole moment of nearly 2 D. Hence, this molecule may form in other mechanisms than those related to glyoxal, and the data in this work should aid in its characterization and potential interstellar observation.

Even though HOCCOH lies 45.8 kcal mol^{-1} above the glyoxal minimum and more than 30 kcal mol^{-1} above the next-highest isomer, this form of $C_2O_2H_2$ has been scrutinized previously through both argon matrix experiments and supporting quantum chemically computed vibrational frequencies at the MP2/6-31G* level of theory.[90] The frequencies of this alkyne-diol are given in Table 9. The two argon-matrix classified fundamental frequencies, unsurprisingly, correspond to the two most intense fundamentals, ν_2 and ν_6, b-irrep motions involving the O-H stretches and C-O-H bends, respectively. While the argon matrix ν_2 is in line with what a matrix shift (~ 44 cm^{-1}) should produce compared to gas phase data for this energy regime around 3600 cm^{-1}, the F12-TcCR+DZ ν_6 bend at 1204.8 cm^{-1} is below the experimental value of 1212.4 cm^{-1}. Regardless, the quantum chemical values and the argon matrix are sufficiently close for the remaining anharmonic frequencies to be taken as trustworthy. The high frequency O-H stretches are nearly degenerate with one another implying that their intensities will actually enhance the total signal in this range. These frequencies at 3630-3632 cm^{-1} are in line with what are expected for alcohol O-H stretches and are computed to be within 5.0 cm^{-1} of the related ethynol (HCCOH) molecule. Peaks at 1338.8 cm^{-1} and, again, 1204.8 cm^{-1} should be observable.

Additionally, the CCSD(T)-F12b/cc-pCVTZ barrier to planarity is a meager 1.73 kcal mol^{-1} or just 605 cm^{-1} showcasing the

Table 9 Vibrational frequencies (in cm^{-1}) of HOCCOH with B3LYP/aug-cc-pVTZ intensities (in km mol^{-1})

Mode	Description	F12-TcCR	F12-TcCR+DZ	f	Expt.
ω_1 (a)	Sym. O−H Stretch	3824.6	3824.6	54	
ω_2 (b)	Anti-Sym. O−H Stretch	3823.0	3823.0	177	
ω_3 (a)	C−C Stretch	2442.7	2442.7	1	
ω_4 (b)	C−O−H Bend	1378.0	1378.0	73	
ω_5 (a)	C−O−H Bend	1285.3	1285.3	1	
ω_6 (b)	C−O−H Bend	1250.3	1250.3	401	
ω_7 (a)	C−O Stretch	802.5	802.5	1	
ω_8 (a)	O−C−C Bend	361.3	361.3	1	
ω_9 (b)	O−C−C Bend	353.3	353.3	3	
ω_{10} (a)	Torsion	281.3	281.3	133	
ω_{11} (a)	O−C−C Bend	235.1	235.1	1	
ω_{12} (b)	O−C−C Bend	231.5	231.5	17	
ν_1 (a)	Sym. O−H Stretch	3631.1	3631.5	45	
ν_2 (b)	Anti-Sym. O−H Stretch	3628.7	3630.1	158	3586.2[a]
ν_3 (a)	C−C Stretch	2363.6	2360.1	1	
ν_4 (b)	C−O−H Bend	1344.8	1338.8	84	
ν_5 (a)	C−O−H Bend	1239.1	1243.7	1	
ν_6 (b)	C−O−H Bend	1232.7	1204.8	377	1212.4[a]
ν_7 (a)	C−O Stretch	808.6	809.3	1	
ν_8 (a)	O−C−C Bend	287.5	350.5	13	
ν_9 (b)	O−C−C Bend	309.0	316.8	3	
ν_{10} (a)	Torsion	214.3	215.0	55	
ν_{11} (a)	O−C−C Bend	283.5	246.3	63	
ν_{12} (b)	O−C−C Bend	230.3	169.8	19	
$\nu_1 + \nu_2$			7078.3	26	

Previous argon matrix data from Ref. 90

Table 10 Rotational Constants and Dipole Moment (F12-TZ) of HOCCOH

Const.	Units	F12-TcCR	F12-TcCR+DZ
A_e	MHz	324948.2	324948.2
B_e	MHz	3679.2	3679.2
C_e	MHz	3675.6	3675.6
A_0	MHz	324138.4	324137.8
B_0	MHz	3675.9	3677.1
C_0	MHz	3666.1	3666.8
Δ_J	Hz	349.613	349.613
Δ_K	MHz	98.151	98.147
Δ_{JK}	kHz	70.952	70.993
δ_J	mHz	−864.485	−865.282
δ_K	MHz	1.360	1.360[a]
Φ_J	μHz	8.356	9.481
Φ_K	MHz	−7.185	−7.189
Φ_{JK}	mHz	169.499	194.597
Φ_{KJ}	kHz	−2.480	−2.474
ϕ_j	μHz	−2.826	−2.332
ϕ_{jk}	Hz	2.002	2.079
ϕ_k	kHz	−993.573	−991.122[b]
μ	D	2.03	
κ		−0.9999	

[a]Within the S-reduced Hamiltonian, $d_2 = -1.919$ Hz.
[a]Within the S-reduced Hamiltonian, $h_3 < 1$ mHz.

torsion to be a large-amplitude motion. Such an energy is above all of the heavy atom bends and the torsion in Table 10 implying that VPT2 will not be sufficient for providing spectroscopically-accurate results.[74,79,91] However, the six-lowest energy fundamental frequencies are either too low in intensity or frequency to be observed astronomically or potentially even in the laboratory rendering such a concern moot for all but the most holistic of spectroscopic characterizations.

The rotational constants for this dipolar molecular isomer are given in Table 10. HOCCOH has a notable dipole moment of 2.03 D even though it is essentially prolate. B_0 and C_0 differ by effectively 10 MHz (3677.1 MHz versus 3666.8 MHz for F12-TcCR+DZ). Whether this molecule plays any role in ice chemistry beyond that which as been reported[21] has yet to be seen, but these data provided here should allow for at least a solid first approximation for building the necessary spectral library for its potential observation. Finally, the strong anharmonicities present in the low-frequency modes for this molecule likely render the VPT2-computed centrifugal distortion constants qualitatively correct at best.

4 Conclusions

Of the five $C_2O_2H_2$ isomers examined herein, *cis*-glyoxal and *cyc*-H_2COCO are tantalizing targets for radioastronomical observation. While these isomers have been detected in interstellar ice analogues recently,[21] *cis*-glyoxal is the most polar. Even though *trans*-glyoxal is the lowest energy, its C_{2h} symmetry defines it to be non-polar. Additionally, the related (Z)-1,2-ethenediol ($C_2O_2H_4$) molecule has recently been observed in the interstellar medium,[49,50] making the *cis* conformer of glyoxal the best target for radioastronomy of the set. However, *cyc*-H_2COCO is only 10.7 kcal mol^{-1} above *cis*-glyoxal. Its structural properties link it to other ketones, epoxides, and oxirenes. *Cyc*-H_2COCO exhibits the second-largest dipole moment (3.31 D), its ν_3 C-O stretch at 1963.0 cm^{-1} is the second-most intense of those examined here, and this fundamental frequency along with its nearly degenerate and nearly as intense $2\nu_8$ overtone falls in an area of the IR that is not heavily laden with PAH features. Hence, it would be a natural target for a combined IR and radioastronomical search.

The total set of vibrational, rotational, and rovibrational spectral data computed in this work will certainly aid in any studies (laboratory or otherwise) of these molecules. They are known to form in simulated interstellar ices making them likely to do so in the interstellar medium. Sublimation events may put these $C_2O_2H_2$ species into the gas phase, and the data provided herein would certainly aid in their detection through JWST, ALMA, or the next generation of telescopes and observatories.[92]

5 Acknowledgements

This work is supported by NASA Grant 22-A22ISFM-0009, the University of Mississippi's College of Liberal Arts, and the Mississippi Center for Supercomputing Research funded in part by NSF Grant OIA-1757220. AGW acknowledges further support from the Barry Goldwater Scholarship and Excellence in Education Foundation. Ally, as we finish your tenth paper here, know that no matter whatever happens in life, you've already made an outsized impact on science and your groupmates. All of us (especially Rebecca, Taylor, Athena, Zach, Brent, and myself) will miss your positive spirit, hard work, soccer matches, and cackle.

Notes and references

1 M. Nuevo, U. J. Meierhenrich, L. d'Hendecourt, G. M. Muñoz Caro, E. Dartois, D. Deboffle, W. H. P. Theimann, J.-H. Bredehoeft and L. Nahon, *Adv. Space Res.*, 2007, **39**, 400–404.

2 C. K. Materese, M. Nuevo, P. P. Bera, T. J. Lee and S. A. Sandford, *Astrobiology*, 2013, **13**, 948–962.

3 E. F. van Dishoeck, E. Herbst and D. A. Neufeld, *Chem. Rev.*, 2013, **113**, 9043–9085.

4 B. M. Jones, R. I. Kaiser and G. Strazzulla, *Astrophys. J.*, 2014, **788**, 170.

5 S. Ioppolo, Z. Kanuchová, R. L. James, A. Dawes, A. Ryabov, J. Dezalay, N. C. Jones, S. V. Hoffmann, N. J. Mason and G. Strazzulla, *Astron. Astrophys.*, 2021, **646**, A172.

6 S. A. Sandford, M. Nuevo, P. P. Bera and T. J. Lee, *Chem. Rev.*, 2020, **120**, 4616–4659.

7 E. Herbst, *Chem. Rev.*, 2013, **113**, 8707–8709.

8 O. H. Wilkins and G. A. Blake, *Astrochemistry*, American Chemical Society, Washington, DC, USA, 2021.

9 A. G. G. M. Tielens, *Molecular Astrophysics*, Cambridge University Press, Cambridge, UK, 2021.

10 B. A. McGuire, *Astrophys. J. Suppl. Ser.*, 2018, **239**, 17.

11 B. A. McGuire, *Astrophys. J. Suppl. Ser.*, 2021, **259**, 30.

12 R. T. Garrod, S. L. W. Weaver and E. Herbst, *Astrophys. J.*, 2008, **682**, 283.

13 V. Wakelam, I. W. M. Smith, E. Herbst, J. Troe, W. Geppert, H. Linnartz, K. Öberg, E. Roueff, M. Agúndez, P. Pernot, H. Cuppen, J. Loison and D. Talbi, *Space Sci. Rev.*, 2010, **156**, 13–72.

14 K. I. Öberg, *Chem. Rev.*, 2016, **116**, 9631–9663.

15 Clément, A., Taillard, A., Wakelam, V., Gratier, P., Loison, J.-C., Dartois, E., Dulieu, F., Noble, J. A. and Chabot, M., *Astron. Astrophys.*, 2023, **675**, A165.

16 C. Zhu, N. F. Kleimeier, A. M. Turner, S. K. Singh, R. C. Fortenberry and R. I. Kaiser, *Proc. Natl. Acad. Sci. U.S.A.*, 2021, **119**, e2111938119.

17 S. K. Singh, C. Zhu, J. L. Jeunesse, R. C. Fortenberry and R. I. Kaiser, *Nature Comm.*, 2022, **13**, 375.

18 R. C. Fortenberry, R. I. Kaiser and R. J. McMahon, *J. Phys. Chem. A*, 2022, **126**, 6571–6574.

19 M. J. Abplanalp, S. Góbi, A. Bergantini, A. M. Turner and R. I. Kaiser, *Chem. Phys. Chem.*, 2018, **19**, 556–560.

20 N. F. Kleimeier, A. M. Turner, R. C. Fortenberry and R. I. Kaiser, *Chem. Phys. Chem.*, 2020, **21**, 1531–1540.

21 J. Wang, A. M. Turner, J. H. Marks, C. Zhang, N. F. Kleimeier, A. Bergantini, S. K. Singh, R. C. Fortenberry and R. I. Kaiser, *Astrophys. J.*, 2024, **967**, 79.

22 A. M. Turner, A. S. Koutsogiannis, N. F. Kleimeier, A. Bergantini, C. Zhu, R. C. Fortenberry and R. I. Kaiser, *Astrophys. J.*, 2020, **896**, 88.

23 A. R. H. Cole and G. A. Osborne, *Spectrochim. Acta*, 1971, **27**,

2461–2490.
24 W. Holzer and D. A. Ramsay, *Canadian J. Phys.*, 1970, **48**, 1759–1765.
25 R. K. Harris, *Spectrochim. Acta*, 1963, **20**, 1129–1141.
26 F. W. Birssa, J. M. Brown, A. R. H. Cole, A. Lofthus, S. L. N. G. Kirshnamachari, G. A. Osborne, J. Paldus, D. A. Ramsay and L. Watmann, *Canadian J. Phys.*, 1970, **48**, 1230–1241.
27 H. Hübner, A. Leeser, A. Burkert, D. A. Ramsay and W. Hüttner, *J. Mol. Spectrosc*, 1997, **184**, 221–236.
28 J. D. Dallas, B. R. Westbrook and R. C. Fortenberry, *Front. Astron. Space Sci.*, 2021, **7**, 626407.
29 H.-Y. Jian, C.-T. Yang and L.-K. Chu, *Phys. Chem. Chem. Phys.*, 2021, **23**, 14699–14705.
30 M. C. Davis, N. R. Garrett and R. C. Fortenberry, *Phys. Chem. Chem. Phys.*, 2022, **24**, 18552–18558.
31 J. H. Marks, J. Wang, R. C. Fortenberry and R. I. Kaiser, *Proc. Natl. Acad. Sci. U.S.A.*, 2022, **119**, e2217329119.
32 A. G. Watrous, B. R. Westbrook and R. C. Fortenberry, *Mon. Not. Royal Astron. Soc.*, 2024, **527**, 11090–11094.
33 I. M. Mills, *Molecular Spectroscopy - Modern Research*, Academic Press, New York, 1972, pp. 115–140.
34 D. Papousek and M. R. Aliev, *Molecular Vibration-Rotation Spectra*, Elsevier, Amsterdam, 1982.
35 J. K. G. Watson, *Vibrational Spectra and Structure*, Elsevier, Amsterdam, 1977, pp. 1–89.
36 P. R. Franke, J. F. Stanton and G. E. Douberly, *J. Phys. Chem. A*, 2021, **125**, 1301–1324.
37 C. Puzzarini, *Int. J. Quantum Chem.*, 2016, **117**, 129–138.
38 M. Biczysko, J. Bloino and C. Puzzarini, *WIREs Comput. Mol. Sci.*, 2018, **8**, e1349.
39 R. C. Fortenberry and T. J. Lee, *Ann. Rep. Comput. Chem.*, 2019, **15**, 173–202.
40 R. C. Fortenberry and T. J. Lee, *Vibrational Dynamics of Molecules*, World Scientific, Singapore, 2022, pp. 235–295.
41 C. Puzzarini and J. F. Stanton, *Phys. Chem. Chem. Phys.*, 2023, **25**, 1421.
42 R. C. Fortenberry, X. Huang, J. S. Francisco, T. D. Crawford and T. J. Lee, *J. Chem. Phys.*, 2012, **136**, 234309.
43 L. Bizzocchi, V. Lattanzi, J. Laas, S. Spezzano, B. M. Giuliano, D. Prudenzano, C. Endres, O. Sipilä and P. Caselli, *Astron. Astrophys.*, 2017, **602**, A34.
44 R. A. Theis and R. C. Fortenberry, *Mol. Astrophys.*, 2016, **2**, 18–24.
45 J. P. Wagner, D. C. McDonald II and M. A. Duncan, *Angew. Chem. Int. Ed*, 2018, **57**, 5081–5085.
46 R. C. Fortenberry and J. S. Francisco, *Astrophys. J.*, 2017, **835**, 243.
47 A. Fuente, J. R. Goicoechea, J. Pety, R. L. Gal, R. Martín-Doménech, P. Gratier, V. Guzmán, E. Roueff, J. C. Loison, G. M. M. Caro, V. Wakelam, M. Gerin, P. Riviere-Marichalar and T. Vidal, *Astrophys. J. Lett*, 2017, **851**, 49.
48 S. Nickerson, N. Rangwala, S. W. J. Colgan, C. DeWitt, X. Huang, K. Acharyya, M. Drozdovskaya, R. C. Fortenberry, E. Herbst and T. J. Lee, *Astrophys. J.*, 2021, **907**, 51.
49 M. Melosso, L. Bizzocchi, H. Gazzeh, F. Tonolo, J.-C. Guillemin, S. Alessandrini, V. M. Rivlla, L. Dore, V. Barone and C. Puzzarini, *Phys. Chem. Chem. Phys.*, 2022, **58**, 2750–2753.
50 V. M. Rivilla, L. Colzi, I. Jiménez-Serra, J. Martín-Pintado, A. Megías, M. Melosso, L. Bizzocchi, Álvaro López-Gallifa, A. Martínez-Henares, S. Massalkhi, B. Tercero, P. de Vicente, J.-C. Guillemin, J. G. de la Concepción, F. Rico-Villas, S. Zeng, S. Martín, M. A. Requena-Torres, F. Tonolo, S. Alessandrini, L. Dore, V. Barone and C. Puzzarini, *Astrophys. J. Lett.*, 2022, **929**, L11.
51 K. Raghavachari, G. W. Trucks, J. A. Pople and M. Head-Gordon, *Chem. Phys. Lett.*, 1989, **157**, 479–483.
52 T. D. Crawford and H. F. Schaefer III, *Reviews in Computational Chemistry*, Wiley, New York, 2000, vol. 14, pp. 33–136.
53 I. Shavitt and R. J. Bartlett, *Many-Body Methods in Chemistry and Physics: MBPT and Coupled-Cluster Theory*, Cambridge University Press, Cambridge, 2009.
54 T. Helgaker, T. A. Ruden, P. Jørgensen, J. Olsen and W. Klopper, *J. Phys. Org. Chem.*, 2004, **17**, 913–933.
55 T. B. Adler, G. Knizia and H.-J. Werner, *J. Chem. Phys.*, 2007, **127**, 221106.
56 G. Knizia, T. B. Adler and H.-J. Werner, *J. Chem. Phys.*, 2009, **130**, 054104.
57 H.-J. Werner, P. J. Knowles, G. Knizia, F. R. Manby and M. Schütz, *WIREs Comput. Mol. Sci.*, 2012, **2**, 242–253.
58 H.-J. Werner, P. J. Knowles, F. R. Manby, J. A. Black, K. Doll, A. Heßelmann, D. Kats, A. Köhn, T. Korona, D. A. Kreplin, Q. Ma, T. F. Miller, A. Mitrushchenkov, K. A. Peterson, I. Polyak, G. Rauhut and M. Sibaev, *WIREs Comput. Mol. Sci.*, 2022.
59 K. A. Peterson, T. B. Adler and H.-J. Werner, *J. Chem. Phys.*, 2008, **128**, 084102.
60 B. R. Westbrook and R. C. Fortneberry, *J. Chem. Theory Comput.*, 2023, **19**, 2606–2615.
61 M. Douglas and N. Kroll, *Ann. Phys.*, 1974, **82**, 89–155.
62 A. G. Watrous, B. R. Westbrook and R. C. Fortenberry, *J. Phys. Chem. A*, 2021, **125**, 10532–10540.
63 J. F. Gaw, A. Willets, W. H. Green and N. C. Handy, *Advances in Molecular Vibrations and Collision Dynamics*, JAI Press, Inc., Greenwich, Connecticut, 1991, pp. 170–185.
64 A. G. Watrous, B. R. Westbrook and R. C. Fortenberry, *Int. J. Quant. Chem.*, 2023, **123**, e27225.
65 X. Huang and T. J. Lee, *J. Chem. Phys.*, 2008, **129**, 044312.
66 X. Huang and T. J. Lee, *J. Chem. Phys.*, 2009, **131**, 104301.
67 X. Huang, P. R. Taylor and T. J. Lee, *J. Phys. Chem. A*, 2011, **115**, 5005–5016.
68 M. B. Gardner, B. R. Westbrook, R. C. Fortenberry and T. J. Lee, *Spectrochim. Acta A*, 2021, **248**, 119184.
69 A. D. Becke, *J. Chem. Phys.*, 1993, **98**, 5648–5652.
70 W. T. Yang, R. G. Parr and C. T. Lee, *Phys. Rev. A*, 1986, **34**, 4586–4590.
71 C. Lee, W. T. Yang and R. G. Parr, *Phys. Rev. B.*, 1988, **37**, 785–789.

72 T. H. Dunning, *J. Chem. Phys.*, 1989, **90**, 1007–1023.

73 M. J. Frisch, G. W. Trucks, H. B. Schlegel, G. E. Scuseria, M. A. Robb, J. R. Cheeseman, G. Scalmani, V. Barone, G. A. Petersson, H. Nakatsuji, X. Li, M. Caricato, A. V. Marenich, J. Bloino, B. G. Janesko, R. Gomperts, B. Mennucci, H. P. Hratchian, J. V. Ortiz, A. F. Izmaylov, J. L. Sonnenberg, D. Williams-Young, F. Ding, F. Lipparini, F. Egidi, J. Goings, B. Peng, A. Petrone, T. Henderson, D. Ranasinghe, V. G. Zakrzewski, J. Gao, N. Rega, G. Zheng, W. Liang, M. Hada, M. Ehara, K. Toyota, R. Fukuda, J. Hasegawa, M. Ishida, T. Nakajima, Y. Honda, O. Kitao, H. Nakai, T. Vreven, K. Throssell, J. A. Montgomery, Jr., J. E. Peralta, F. Ogliaro, M. J. Bearpark, J. J. Heyd, E. N. Brothers, K. N. Kudin, V. N. Staroverov, T. A. Keith, R. Kobayashi, J. Normand, K. Raghavachari, A. P. Rendell, J. C. Burant, S. S. Iyengar, J. Tomasi, M. Cossi, J. M. Millam, M. Klene, C. Adamo, R. Cammi, J. W. Ochterski, R. L. Martin, K. Morokuma, O. Farkas, J. B. Foresman and D. J. Fox, *Gaussian 16 Revision C.01*, 2016, Gaussian Inc. Wallingford CT.

74 Q. Yu, J. M. Bowman, R. C. Fortenberry, J. S. Mancini, T. J. Lee, T. D. Crawford, W. Klemperer and J. S. Francisco, *J. Phys. Chem. A*, 2015, **119**, 11623–11631.

75 B. Finney, R. C. Fortenberry, J. S. Francisco and K. A. Peterson, *J. Chem. Phys.*, 2016, **145**, 124311.

76 A. Karton and D. Talbi, *Chem. Phys.*, 2014, **436-437**, 22–28.

77 W. Györffy and H.-J. Werner, *J. Chem. Phys.*, 2018, **148**, 114104.

78 C. Z. Palmer, R. A. Firth and R. C. Fortenberry, *J. Comput. Chem.*, 2024.

79 R. C. Fortenberry, *J. Phys. Chem. Lett.*, 2024.

80 B. R. Westbrook and R. C. Fortenberry, *J. Phys. Chem. A*, 2020, **124**, 3191–3204.

81 A. G. G. M. Tielens, in *25 Years of PAH Hypothesis*, EDP Sciences, 2021, pp. 1–10.

82 X. Huang, R. C. Fortenberry and T. J. Lee, *Astrophys. J. Lett.*, 2013, **768**, 25.

83 P. Botschwina, C. Stein, P. Sebald, B. Schröder and R. Oswald, *Astrophys. J.*, 2014, **787**, 72.

84 S.-Y. Chen and Y.-P. Lee, *J. Chem. Phys.*, 2010, **132**, 114303.

85 D. E. Milligan and M. E. Jacox, *J. Chem. Phys.*, 1962, **36**, 2911–2917.

86 B. A. McGuire, P. B. Carroll, R. A. Loomis, I. A. Finneran, P. R. Jewell, A. J. Remijan and G. A. Blake, *Science*, 2016, **352**, 1449–1452.

87 H. Hou, A. Li, H. Hu, Y. Li and B. Wang, *J. Chem. Phys*, 2005, **122**, 224304.

88 B. E. Turner, *Astrophys. J.*, 1977, **213**, L75–L79.

89 M. Agúndez, J. Cernicharo and M. Guélin, *Astron. Astrophys.*, 2015, **577**, L5.

90 G. Maier and C. Rohr, *Liebigs Ann.*, 1996, **1996**, 307–309.

91 R. C. Fortenberry, Q. Yu, J. S. Mancini, J. M. Bowman, T. J. Lee, T. D. Crawford, W. F. Klemperer and J. S. Francisco, *J. Chem. Phys.*, 2015, **143**, 071102.

92 R. C. Fortenberry, *ACS Phys. Chem. Au*, 2023, **4**, 31–39.

The data supporting this article have been included as part of the Supplementary Information.